



**HAL**  
open science

## A microstrip resonator based sensor for GHz characterization of in vitro cell culture

Florian Kölbl, N Boulboul, M Commereuc, E Bourdel

### ► To cite this version:

Florian Kölbl, N Boulboul, M Commereuc, E Bourdel. A microstrip resonator based sensor for GHz characterization of in vitro cell culture. 12th International Conference On Sensing Technology (ICST 2018), Dec 2018, Limerick, Ireland. hal-01985834

**HAL Id: hal-01985834**

**<https://hal.science/hal-01985834v1>**

Submitted on 18 Jan 2019

**HAL** is a multi-disciplinary open access archive for the deposit and dissemination of scientific research documents, whether they are published or not. The documents may come from teaching and research institutions in France or abroad, or from public or private research centers.

L'archive ouverte pluridisciplinaire **HAL**, est destinée au dépôt et à la diffusion de documents scientifiques de niveau recherche, publiés ou non, émanant des établissements d'enseignement et de recherche français ou étrangers, des laboratoires publics ou privés.

# A microstrip resonator based sensor for GHz characterization of *in vitro* cell culture

F. Kölbl, N. Boulboul, M. Commereuc, E. Bourdel  
 Laboratoire ETIS, UMR 8051, ENSEA - U. Paris Seine - U. de Cergy-Pontoise - CNRS  
 6 avenue du Ponceau  
 95014 - Cergy CEDEX - France  
 Email: florian.kolbl@ensea.fr

**Abstract**—This contribution describes a sensor for GHz characterization of *in vitro* cell culture, that overcomes the limitation in high frequency of classical bio-impedance spectroscopy. The sensor we developed enables to monitor a thin layer of approximatively  $30\mu m$  of cells in their liquid culture medium for a relative permittivity in the range of 5 to 55. Here, we demonstrate the measurement principle using a Finite Element model, which has been validated with experimental response. Our sensor has a minimal sensitivity of  $0.3MHz$ . We also used a multiphysics model to demonstrate that this technology does not affect tissue safety for input power level compatible with a sufficient measurement signal on noise ratio. This technology will be used in experiments aiming at the exploration of biomarkers for post-implantation inflammatory reactions of active devices.

## I. INTRODUCTION

Bio-impedance spectroscopy is a measurement technique associated with different applications such as body fluid volume measurement [1], physiological imaging of organs [2] or medical diagnostic as in [3] for instance. The possibility of embedding measurement circuits, makes it a good candidate to obtain biomarkers for many pathologies associated with long term evolution of active implanted devices such as fibrosis or gliosis [4]. In this case the change of the electrode impedance in time is linked with the surrounding tissue evolution and the growth of fibroblast. However, if experimental approaches as [5] have highlighted the possibility of impedance monitoring to detect chronic evolution, there is no quantitative marker of any physiologic reaction up until now.

As illustrated in Fig. 1, the frequency dependence of the complex permittivity  $\epsilon$  of a biological tissue sample (with  $\epsilon'$  the real part and  $\epsilon''$  the imaginary part) can be subdivided into 4 frequency bands [6]. The  $\alpha$  and  $\beta$  bands are linked to relaxations caused by cells membranes and organelles. The  $\delta$  and  $\gamma$  band are associated with molecular and ionic relaxation phenomena. Measurements performed with impedance spectroscopy have a practical limitation in high frequency around few tens or hundreds of  $MHz$ , due to electrode cable-access crosstalk, parasitic capacitances and measurement circuits maximum frequencies. Therefore, current techniques used to investigate biomarkers do not include the  $\delta$  and  $\gamma$  relaxations that could provide additional informations to evaluate a physiopathological state.

In this paper, we propose a novel approach to measure the permittivity of biological samples. We focused on *in vitro*

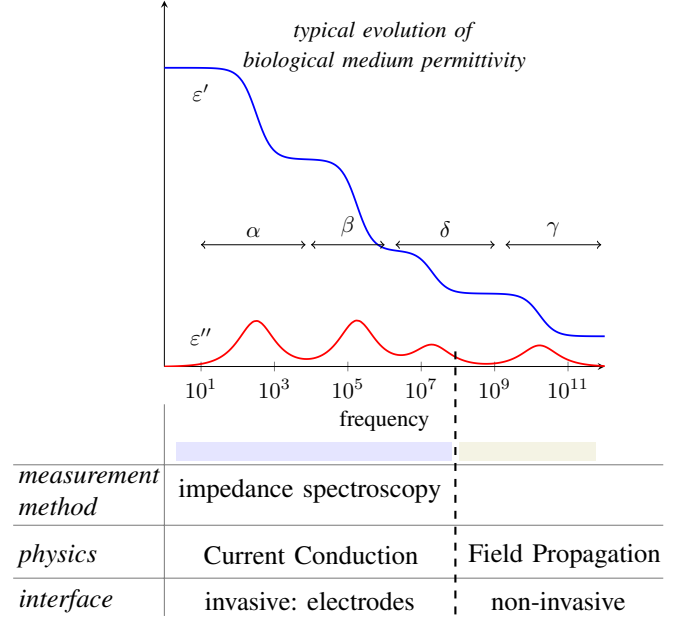


Fig. 1. Typical frequency dependence of the complex permittivity biomaterials (with  $\epsilon'$  the real part and  $\epsilon''$  the imaginary part). 4 bands associated with relaxations can be observed:  $\alpha$ ,  $\beta$ ,  $\delta$  and  $\gamma$ . In low frequency, measurement are performed with invasive electrode, using current conduction to sense the impedance of tissue. In this contribution, to overcome frequency limitation of this technique, we propose to use a field-propagation based technique to sense the permittivity in the  $\delta$  or  $\gamma$  domains.

cell culture as used for investigation of biomarkers associated to fibrosis as described in [5]. Our solution is based on a microstrip resonator, which acts as a non-invasive interface using the electric field propagation to characterize the tissue. In section II, we detail the measurement technique, explain the design of the resonator and expose the challenges faced in the case of *in vitro* measurements. In section III, we explain the models we implemented to assess the viability of the measurement principle and the respect of tissue safety of our sensor. Finally, in section IV, we consider the possibilities of this technology and future challenges to investigate.

## II. DESIGN OF THE RESONATOR

### A. State of the art of High Frequency measurement

In the low frequency domain, the usual quantity under consideration to characterize tissue properties is often the complex impedance of a pair of electrodes separated by

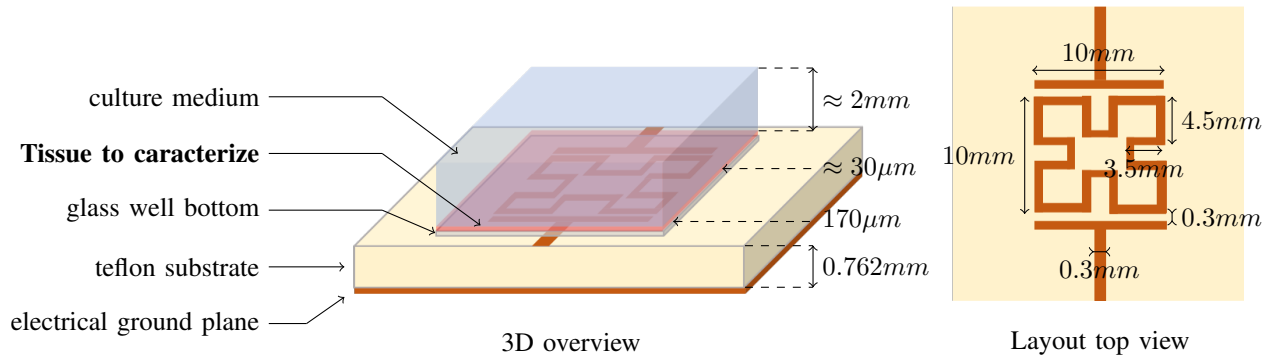


Fig. 2. Geometry of the *in vitro* tissue permittivity sensor proposed: on the left, the 3D overview shows the different layers of materials in the structure; a resonator is designed on a teflon substrate, which is placed under a glass composed culture well; inside the well, cells are located at the bottom of the well forming a thin layer, the culture medium is considered to be located on top, with a much larger thickness. On the right, the layout top view shows the modified Minkowski resonator shape we used for the microstrip resonator structure.

the tissue sample [4], [5]. However, at high frequency the physics only allows to measure the complex permittivity; both quantities are directly linked [7].

Permittivity measurements can be performed with different methods [8]: with a resonant cavity for high accuracy however this technique suppose manipulation of the sample, or with free-space method or transmission lines and resonant structures. The last method has already been used for measurement over chemical [9] or biological samples [10], [11]. In this case a resonant structure is loaded with the material under consideration, and the shift in the resonance frequency is correlated to the effective permittivity over the sensor.

### B. Resonator design

We designed a structure to adapt to a culture well suitable for *in vitro* myofibroblast. This device also enables optical measurement for latter experiments (*Ibidi -  $\mu$ -Slide 2 Well Glass Bottom*). Different structures of resonator can be found in the literature, the most commonly used shape is based on a ring resonator [10], [11]. The length of the resonator perimeter is directly linked to the resonance wavelength; in the case of a *in vitro* culture, cells will agglutinate around the place they are deposited, i.e. from the center of the well. As a consequence the smaller the structure, the more reliable the measure will be as the cell layer will be almost homogeneous over the structure. We chose a less regular shape compared to ring resonator in order to minimize the area for a given resonance frequency.

We used a structure presented in Fig. 2, based on a modified Minkowski shape [12]. We fixed the first resonance at  $4GHz$ , in the range of the transition from  $\delta$  to  $\gamma$  bands. The resonator was built on a Teflon substrate ( $\epsilon_r = 2.55$ ) at a thickness of  $.762mm$ . The overall surface area of the sensor is around  $1cm^2$ . The access microstrip port were matched to an impedance of  $50\Omega$ .

### C. Preliminary results and in vitro linked challenges

Preliminary measurement results of the scattering parameters, here the reflection parameter  $S_{11}$ , are exhibited in Fig. 3. Measurement were performed using a *KEYSIGHT M9375A*

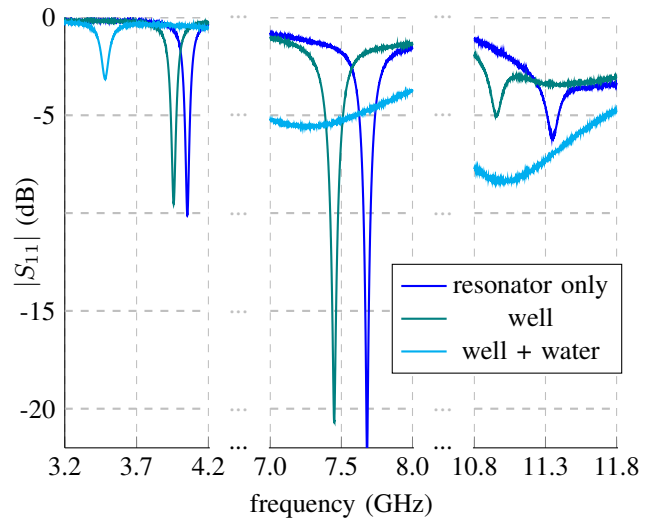


Fig. 3. Sensor reflection scattering parameter  $S_{11}$  measurement for three different situations: 1) teflon resonator only 2) resonator loaded with the empty culture well 3) resonator loaded with the culture well with  $1mL$  of pure water.

network analyzer, with a bandwidth between  $300MHz$  and  $26GHz$ . As depicted in Fig. 3, three resonance frequencies can be observed, the fundamental and the two first harmonic resonances. Figures are summed up in Table I. As a consequence, our device is able to characterize the tissue for the different resonance frequencies. In the rest of the paper, for clarity of the figures and models, we only focus on the first resonance around  $4GHz$ .

We measured the  $S_{11}$  parameter when loading the device:

- with the culture well, with a thickness of glass of  $170\mu m$ ,
- with the culture well and  $1mL$  of pure water (volume corresponding to a layer of  $\approx 2mm$  of liquid in the well, corresponding to *in vitro* culture conditions).

For the observed resonance, adding a material on the top of the substrate decreases the resonance frequency value in the range of few hundreds of  $MHz$ . For a given load, the resonance frequency shift depends on:

TABLE I  
VALUES OF RESONANCE FREQUENCIES FOR VARIOUS LOAD, OBTAINED  
FROM MEASURE AND SIMULATION RESULTS

resonance frequency	#1	#2	#3
<i>Unloaded</i>			
measurement (GHz)	4.054	7.680	11.35
model (GHz)	4.041	7.781	11.54
relative error	$3.2 \cdot 10^{-3}$	$1.3 \cdot 10^{-2}$	$1.7 \cdot 10^{-2}$
<i>loaded with well</i>			
measurement (GHz)	3.958	7.450	10.96
model (GHz)	3.940	7.631	11.31
relative error	$4.5 \cdot 10^{-3}$	$2.4 \cdot 10^{-2}$	$3.2 \cdot 10^{-2}$
<i>loaded with well and water</i>			
measurement (GHz)	3.481	7.282	10.98
model (GHz)	3.470	7.479	not performed
relative error	$3.2 \cdot 10^{-3}$	$2.7 \cdot 10^{-2}$	

- the material real part of the permittivity: the higher the permittivity, the resonance frequency decreases shift increases,
- the temperature: as the complex permittivity depends on temperature, this parameter may affect the measurement. However, for cell culture conditions, it remains stable (here fixed at  $T = 37^\circ C$ ),
- the material layer thickness.

In our case, the permittivity is the quantity of interest. The thickness of the biological layer directly depends on the nature of the cells, however it is always a monolayer. As we were interested in monitoring cultures of myofibroblasts [13], [14], we considered that the thickness will be approximatively  $30\mu m$ .

This layer is extremely thin compared to the surrounding ones of glass and water. Moreover, for biological tissue, the value of  $\epsilon_r$  is expected to be in the range of approximatively 5 to 55 [15], whereas for the culture liquid we can expect a permittivity similar to water [16], approximatively around 137 in the range of few GHz. The challenge is to determine if the permittivity can be observed under such conditions, with chosen structure and without degrading the sample under test.

### III. SENSOR MODELING

As no empirical approach is feasible to mimic a thin layer of variable permittivity, we developed a model to assess our technique. We used Finite Element Method (simulations under *COMSOL, RF module*) to model the full structure of Fig. 2, with both Maxwell and heat equations. In this section, we first detail the validation of our electromagnetic model and we show the results of sensitivity of our resonator. Then, we explain the results obtained from RF-exposure models. Values for the properties of the bio-samples were taken from [15]–[17].

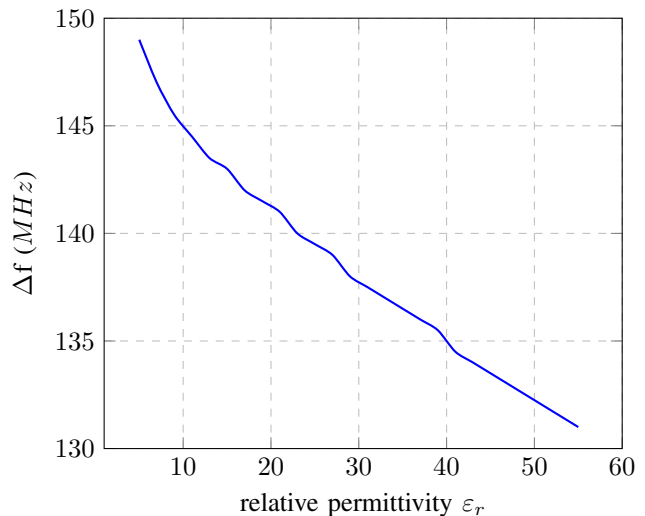


Fig. 4. Evolution of the first resonance  $\Delta f$  for a  $30\mu m$  culture cell layer with a variation of the relative permittivity  $\epsilon_r$  for a conductivity  $\sigma = 0.5 \cdot m^{-1}$ .

#### A. Electromagnetic model

In order to validate the electromagnetic model, we used the measurement performed in Fig. 3 and checked the matching of the resonance frequencies for each situation (without any load - with the well as load - with the well and water as load). The obtained values are summed up in Table I. For the first frequency, here our main focus, the relative error remains under 0.5% in any case. As a consequence, for a fixed cell layer thickness, the future investigation of the resonance frequency shift with variation of the permittivity is likely to be trusted. For the second and third resonances, the error slightly increases; however, it remains under 5%. The overall model is therefore coherent with the observed physical phenomena and accurate around the first resonance, between 3GHz and 4GHz.

To evaluate the permittivity, the practical measurement will be the frequency shift for different loads. Considering the context, we propose to measure the permittivity by focusing on the shift between the sensor loaded with the well and culture medium before introduction of cells, and the sensor with the cells as shown in Fig. 2. This quantity is a function of the culture cell permittivity and will be noted here:

$$\Delta f = f_0|_{well+water} - f_0|_{cells} \quad (1)$$

in Hz where  $f_0$  is the resonance frequency.

The evolution of  $\Delta f$  for the first resonance is shown in Fig. 4. These results were obtained by a parametric sweep of the relative permittivity of the cell layer from 5 to 55. Here, an increase of the permittivity has for consequence a decrease of  $\Delta f$  as the bio-sample under measurement is directly in contact with the liquid layer that has a permittivity in the range of 137. This value is the practical measurement limit, however such a range is unlikely for bio-materials over the GHz [15], [17] as it remains far less than 100. Therefore, our measurement setup is suitable from the application perspective.

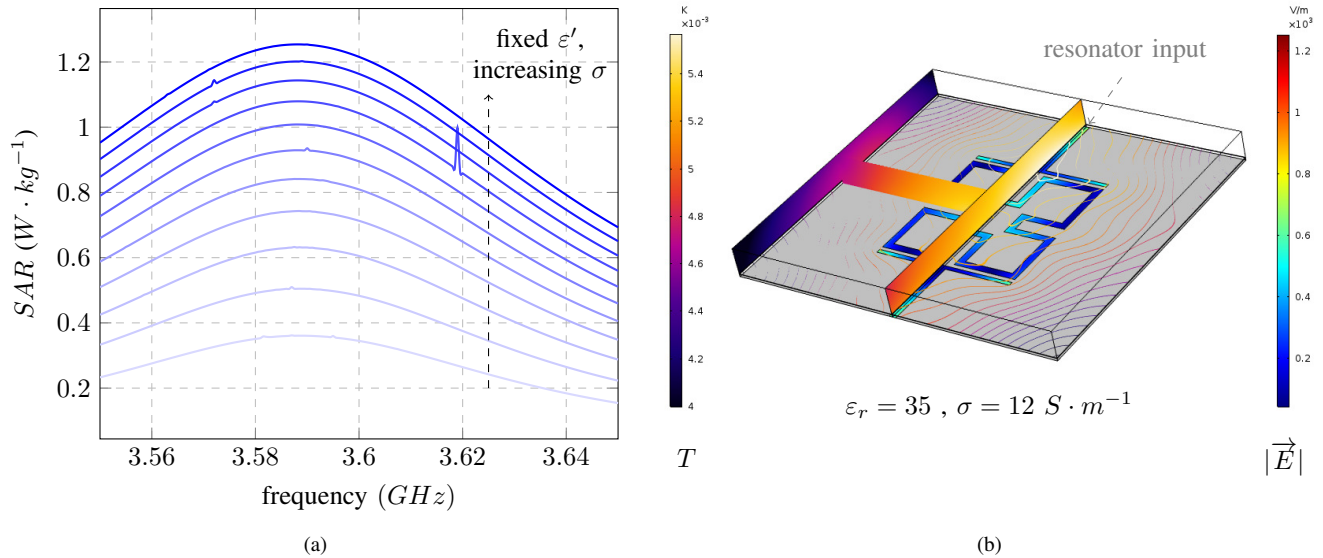


Fig. 5. (a) Specific Absorption Rate ( $SAR$ ) variation with frequency in the culture cell layer for a fixed relative permittivity of  $\epsilon_r = 35$  for different values of conductivities from 2 to  $12 S \cdot m^{-1}$  with a step of  $1 S \cdot m^{-1}$  for an input measurement stimulus of  $-1dBm$  and a tissue density of  $\rho = 1030kg \cdot m^{-3}$  [17] (b) Variation of the magnitude of the electrical field over the microstrip in  $V \cdot m^{-1}$  and of the temperature elevation in  $K$ ; this last quantity is plotted with iso-temperature-surfaces in the culture cell layer and with vertical cross sections for the culture medium. Simulation was performed for the maximal observed SAR, e.g.  $\epsilon_r = 35$  and  $\sigma = 12S \cdot m^{-1}$ , and for a median value of thermal conductivity ( $\lambda = 0.5W \cdot m^{-1} \cdot K^{-1}$ ) [17].

For the range of  $\epsilon_r$  of interest, 5 to 55, the full span of  $\Delta f$  is  $18MHz$ . For relative permittivity values above 10, the curve is quasi linear and the sensitivity of the sensor is  $-0.30MHz$  (as  $\epsilon_r$  is unitless). For lower values, the curve is non-linear and the sensitivity increases up to  $-1MHz$  at  $\epsilon_r = 5$ .

### B. Coupled thermal model

The exposure of even a small amount of resistive material to an electromagnetic field generates heat. We coupled our model with steady state heat equation with a heat source taking into account Joule effect:

$$Q_e = \sigma \vec{E} \cdot \vec{E}^* \quad (2)$$

in  $W \cdot m^{-3}$ , with  $\sigma$  the conductivity in  $S \cdot m^{-1}$ . From equation 2, it is clear that the conductivity of the medium is directly responsible for the heating of culture cells. In order to prevent tissue damages or thermal artefact, we computed the maximal temperature increase. We also computed the Specific Absorption Rate ( $SAR$ ), defined as:

$$SAR = \frac{1}{2} \frac{Q_e}{\rho} \quad (3)$$

in  $W \cdot kg^{-1}$ , with  $\rho$  the tissue density in  $kg \cdot m^{-3}$ . Simulation results are shown in Fig. 5.

The  $SAR$  is displayed in Fig. 5(a). In this plot, the relative permittivity is fixed at  $\epsilon_r = 35$  as this quantity does not influence the electric field magnitude at the resonance. We computed  $SAR$  variation with frequency for conductivity values in the range from 2 to  $12 S \cdot m^{-1}$  corresponding to the range that can be expected from bio-samples, in the range of the  $GHz$  [15]. The input stimulus power is here fixed at

$-1dBm$ . The  $SAR$  is maximal at the resonance frequency, and increases for higher values of conductivity. However, for our values, it never exceeds  $1.3W \cdot kg^{-1}$ , which fits American ( $\leq 1.6W \cdot kg^{-1}$ ) or EU ( $\leq 2W \cdot kg^{-1}$ , IEC 62209-1 : 2016) criteria for  $GHz$  field exposure. The reduction of the input power in our case has a limited impact in term of noise. As an illustration, the measurements exhibited in Fig. 3 were performed with a stimulus of  $-5dBm$  with a sufficient signal on noise ratio.

We computed the thermal heating in Fig. 5(b) for the point of maximum  $SAR$  ( $\epsilon_r = 35$ ,  $\sigma = 12S \cdot m^{-1}$ , at the resonance frequency of  $3.59GHz$ ). The temperature is represented by iso-surfaces in the culture cell layer, and by vertical cross sections in the culture medium layer. The temperature has the highest increase near the discontinuities in the resonator shape, where the field magnitude is maximal. However with an input power of  $-1dBm$ , the temperature increase remains lower than  $5.5 \cdot 10^{-3}K$ , thus ensuring the tissue safety during the measurement.

## IV. CONCLUSION AND PERSPECTIVES

In this paper, we proposed a sensor to monitor the permittivity of a monolayer of an *in vitro* cell culture. The setup is based on a resonator, which is loaded by the tissue under consideration. Contrarily to classical impedance spectroscopy, the method is non-invasive. Furthermore, we demonstrated here above that measurements can be performed without a significant temperature increase, even for a small amount of tissue ( $\approx 1.2 \cdot 10^{-2}g$  with our configuration) exposed to a strong field (in the range of  $10^3V \cdot m^{-1}$  at an input power of  $-1dBm$ , see Fig. 5(b)). This technology is particularly suitable for

measurement over the  $GHz$  as the wavelength decreases under  $30cm$  which enables us to design resonator structures restrained within a surface area of few  $cm^2$  compatible with most of culture wells. Higher frequencies can be reached both with smaller structures and by measurement on harmonic resonance frequencies. Moreover, at such frequencies, the permittivity of the tissue is expected to be lower than the one on the culture medium, ensuring the measurement possibility. The conjunction of these elements allows to consider the proposed technology as a good candidate to overcome the frequency limitation of classical electrode-based impedance spectroscopy and to widen the possibilities of embedded tissue characterization.

This first investigation will be also be completed by experiments with cultures of myofibroblasts as performed in [5] at lower frequency, to demonstrate the performances of our sensors and characterize fibrotic tissues growth over a wide spectrum, from  $10^0 Hz$  to  $10^{10} Hz$ . We also consider further optimizations of the resonator structure to increase the sensitivity of the setup and enhance the detection of small changes in the tissue, as well as investigating the design of the resonator on transparent substrates to combine electrical and optical measurements. Finally, another avenue for this project will be to investigate the possibility of embedding the electronics required to perform automated monitoring of tissue evolution.

#### REFERENCES

- [1] M. Y. Jaffrin and H. Morel, "Body fluid volumes measurements by impedance: A review of bioimpedance spectroscopy (bis) and bioimpedance analysis (bia) methods," *Medical engineering & physics*, vol. 30, no. 10, pp. 1257–1269, 2008.
- [2] D. El Khaled, N. Novas, J.-A. Gazquez, and F. Manzano-Agugliaro, "Dielectric and bioimpedance research studies: A scientometric approach using the scopus database," *Publications*, vol. 6, no. 1, p. 6, 2018.
- [3] C. Seward, M. Skolny, C. Brunelle, M. Asdourian, L. Salama, and A. G. Taghian, "A comprehensive review of bioimpedance spectroscopy as a diagnostic tool for the detection and measurement of breast cancer-related lymphedema," *Journal of surgical oncology*, vol. 114, no. 5, pp. 537–542, 2016.
- [4] J. C. Williams, J. A. Hippensteel, J. Dilgen, W. Shain, and D. R. Kipke, "Complex impedance spectroscopy for monitoring tissue responses to inserted neural implants," *Journal of neural engineering*, vol. 4, no. 4, p. 410, 2007.
- [5] E. De Roux, M. Terosiet, F. Kölbl, J. Chrun, P. Aubert, P. Banet, M. Boissière, E. Pauthe, A. Histace, and O. Romain, "Wireless and portable system for the study of in-vitro cell culture impedance spectrum by electrical impedance spectroscopy," in *Digital System Design (DSD), 2017 Euromicro Conference on*. IEEE, 2017, pp. 456–461.
- [6] S. Grimnes, O. Rikshospitalet, and N. H. P. Schwan, "Interface phenomena and dielectric properties of biological tissue," *Encyclopedia of surface and colloid science*, vol. 20, pp. 2643–2653, 2002.
- [7] D. Miklavcic, N. Pavselj, and F. X. Hart, "Electric properties of tissues," 2006.
- [8] O. Tereshchenko, F. J. K. Buesink, and F. B. J. Leferink, "An overview of the techniques for measuring the dielectric properties of materials," in *General Assembly and Scientific Symposium, 2011 XXXth URSI*. IEEE, 2011, pp. 1–4.
- [9] K. K. Adhikari and N.-Y. Kim, "Ultrahigh-sensitivity mediator-free biosensor based on a microfabricated microwave resonator for the detection of micromolar glucose concentrations," *IEEE Transactions on Microwave Theory and Techniques*, vol. 64, no. 1, pp. 319–327, 2016.
- [10] Z. Ramsarop, S. Rocke, N. Gayapersad, and J. Persad, "Csr-based microwave sensor for noninvasive, continuous monitoring of renal function," in *Antennas & Propagation Conference (LAPC), 2016 Loughborough*. IEEE, 2016, pp. 1–5.
- [11] F. Deshours, G. Alqui, H. Kokabi, K. Rachedi, M. Tlili, S. Hardinata, and F. Koskas, "Improved microwave biosensor for non-invasive dielectric characterization of biological tissues," *Microelectronics Journal*, 2018.
- [12] J. P. Gianvittorio and Y. Rahmat-Samii, "Fractal antennas: A novel antenna miniaturization technique, and applications," *IEEE Antennas and Propagation magazine*, vol. 44, no. 1, pp. 20–36, 2002.
- [13] B. Hinz, S. H. Phan, V. J. Thannickal, A. Galli, M.-L. Bochaton-Piallat, and G. Gabbiani, "The myofibroblast: one function, multiple origins," *The American journal of pathology*, vol. 170, no. 6, pp. 1807–1816, 2007.
- [14] J. Baum and H. S. Duffy, "Fibroblasts and myofibroblasts: what are we talking about?" *Journal of cardiovascular pharmacology*, vol. 57, no. 4, p. 376, 2011.
- [15] S. Gabriel, R. Lau, and C. Gabriel, "The dielectric properties of biological tissues: Ii. measurements in the frequency range 10 hz to 20 ghz," *Physics in medicine & biology*, vol. 41, no. 11, p. 2251, 1996.
- [16] W. Ellison, "Permittivity of pure water, at standard atmospheric pressure, over the frequency range 0–25 thz and the temperature range 0–100 c," *Journal of physical and chemical reference data*, vol. 36, no. 1, pp. 1–18, 2007.
- [17] P. Hasgall, E. Neufeld, M. Gosselin, A. Kligenböck, and N. Kuster, "It is database for thermal and electromagnetic parameters of biological tissues. 2011," *URL: www.itis.ethz.ch/database*, 2015.